Supplementary Material: The quantum paraelectric phase of $SrTiO_3$ from first principles

Dongbin Shin,[1,*] Simone Latini,[1] Christian Schäfer,[1] Shunsuke A. Sato,[2,1]
Umberto De Giovannini,[1,3] Hannes Hübener,[1] and Angel Rubio[1,3,4,†]

[1] *Max Planck Institute for the Structure and Dynamics of Matter and Center for Free Electron Laser Science, 22761 Hamburg, Germany*

[2] *Center for Computational Sciences, University of Tsukuba, Tsukuba 305-8577, Japan*

[3] *Nano-Bio Spectroscopy Group, Departamento de Fisica de Materiales, Universidad del País Vasco UPV/EHU- 20018 San Sebastián, Spain*

[4] *Center for Computational Quantum Physics (CCQ), The Flatiron Institute, 162 Fifth avenue, New York NY 10010.*

DEFINITION OF EIGENVECTOR AND EFFECTIVE MASS OF FES PHONON

We evaluated the eigenvector of FES phonon from the difference of the atomic geometries between the optimized paraeletric and ferroelectric tetragonal structure. In formulas the eigenvector of the FES mode can be written as:

$$\mathbf{U}_I^{fes} = \frac{\tau_I^{ferro} - \tau_I^{para}}{\sum_J |\tau_J^{ferro} - \tau_J^{para}|}, \tag{1}$$

where U_I and τ_I are the eigenvector of the FES mode and the position vector for the atom I respectively. For the HSE hybrid functional, we used the same eigenvector and mass of the FES mode evaluated from PBE functional since performing a geometry optimization with the HSE functional is too computationally expensive. Because LDA functional provides paraelectric geometry without strain, eigenvector for the LDA functional is evaluated from DFPT calculation. With this eigenvector, we distorted atomic geometry and evaluated phonon displacement Q_{f} from the position difference between the Ti atom and one of the O atom located in the in-plane section of the octahedron: $Q_{\mathrm{f}} = \tau_{Ti}^z - \tau_{O_{in}}^z$. The effective mass of FES mode is defined as follows $M_f^{eff} = \sum_I M_I \frac{U_I^z}{U_{Ti}^z - U_{O_{in}}^z}$. With similar definitions, we evaluated the FES phonon frequency with the LDA functional, which provides parabolic potential energy surface of FES mode. While the potential energy surface of LDA shows anharmonic behavior with large Q_{f}, the frequency near the paraelectric equilibrium geometry evaluated by fitting parameter is 2.6 THz, which value is comparable result with DFPT calculation (2.4 THz).

SOLVING SCHRÖDINGER EQUATION IN NUMERICAL GRID

To understand the quantum fluctuation and elastic effect in $SrTiO_3$, we solved the 2D lattice Schrödinger equation with fitted potential energy surface from density functional theory calculation. The Hamiltonian for 2D lattice is given as follows: $\hat{H}_{\mathrm{2D}}^{\mathrm{FES,c}} = \hat{P}_f^2/2M_f + \hat{P}_c^2/2M_c + \hat{V}_{2D}^{\mathrm{FES,c}}$. To evaluate the ground and excited states, we exactly diagonalized the Hamiltonian with numerical grid. The 80×80 numerical grid is employed and its convergence is checked up to 160×160. The kinetic matrix for the numerical grid basis set is constructed by discrete variable representation with an uniform grid [1].

FITTING COEFFICIENTS OF 2D POTENTIAL

In our study, we solved the 2D Schrödinger equation with a 2D FES-lattice potential energy surface. To evaluate this 2D potential energy surface, we calculate DFT total energy $E^{2D}_{DFT}[Q_{\rm f}, Q_{\rm c}]$ by distorting the atomic geometry along the FES mode, parameterized by $Q_{\rm f}$ and the c-axis, parameterized by $Q_{\rm c}$. The fitting coefficients of the potential energy surface ($V^{2D}[Q_{\rm f}, Q_{\rm c}] = E^{2D}_{DFT}[Q_{\rm f}, Q_{\rm c}] - E^{2D}_{DFT}[0, 0]$) are evaluated up to the 12th order for $Q_{\rm f}$ and 5th order for $Q_{\rm c}$ as follows:

$$\begin{aligned}\hat{V}^{\rm 2D}[Q_{\rm f}, Q_{\rm c}] = &\sum_{i=1}^{6} k_{f,i}\hat{Q}_f^{2i} + \sum_{j=2}^{5} k_{c,j}\hat{Q}_c^{j} \\ &+ \sum_{i=1}^{6}\sum_{j=1}^{5} k_{fc,i,j}\hat{Q}_f^{2i}\hat{Q}_c^{j}\end{aligned} \tag{2}$$

We found that this high order fitting coefficients reproduces almost identical potential energy surface comparing with the potential energy surface obtained by DFT calculation. The evaluated fitting coefficients are summarized in Table S2, S3, S4 and S5 for various functionals.

LATTICE MASS DEPENDENCY OF FREQUENCY OF FERROELETRIC SOFT MODE

The definition of lattice mass is not clear and the fictitious lattice mass is suggested for the dynamics [2]. To understand the dependency of lattice mass on the frequency of FES mode, we evaluate its frequency with various lattice mass from total cell mass (M_{tot}) to near zero value ($0.02M_W$), when the M_W is Wentzcovitch-type fictitious mass, as shown in Fig S2. This result indicates that the frequency of FES mode is not quite sensitive in the range between total cell mass (M_{tot}) and Wentzcovitch-type fictitious mass (M_W).

MODIFIED LATTICE PARAMETER BY QUANTUM FLUCTUATION AND ELASTIC EFFECT

The description of quantum fluctuation provides the elongated lattice lattice parameter. We summarize the lattice parameter of tetragonal $SrTiO_3$ as shown in Table S6. The lattice c^{2D} in the tetragonal $SrTiO_3$ is increased by quantum fluctuation and nonlinear interaction with ferroeletric soft mode. It is notable that the HSE06 functional provide the comparable values with experimental observation.

TEMPERATURE DEPENDENCY OF FREQUENCY OF FES MODE IN CLASSICAL APPROACHES

To verify whether PBE functional provides realistic potential energy surface comparing with experimetnal observation, we calculated the frequency of FES mode at high temperature using *ab initio* molecular dynamics (AIMD). For the AIMD simulation, we evaluated several independent trajectories with the temperature controlled by a thermostat. To allow enough degrees of freedom, we employed $2 \times 2 \times 2$ supercell. For the time propagation, cell variation is considered for each time step ($\Delta t = 4.8$ fs) and $4 \times 4 \times 4$ and $\mathbf{k}$-point sampling is employed. To determine the frequency of FES mode, we selected the frequency corresponding to the peak for each trajectory and evaluated the average and standard derivation. As shown in main text Fig. 3(a), the AIMD simulation results are consistent with experimental observations. This result indicates that PBE functional provides realistic potential energy surface for the FES mode as experiment.

We also investigated the temperature dependence of FES mode frequency by solving Newton equation with the same 2D potential energy surface as in the quantum calculations. We evaluated the average of multi-trajectories ($N_{traj} = 10^6$) with infinitesimal initial kicking at $t = 0^-$, whose initial geometries are prepared with a thermostat for a given temperature. To determine the frequency of FES mode, we calculated a weighted average using the response function ($\omega(T) = \frac{\int \omega Q_{\mathrm{f}}(\omega,T) d\omega}{\int Q_{\mathrm{f}}(\omega,T) d\omega}$) which is obtained from the time-profile multi-trajectory response ($Q_{\mathrm{f}}(t,T) = \sum_i^{N_{traj}} Q_{f,i}(t,T)/N_{traj}$) to the initial kicking. As shown in Fig. S3(a), the frequency of FES mode in the classical description with 2D potential energy surface provides comparable values with its quantum description at high temperature (~ 300 K). Because the

classical dynamics describes the oscillation inside one of the two wells at low temperature, the FES mode is much stiffer than the one predicted by the quantum description.

EFFECT OF THERMAL LATTICE ON THE TEMPERATURE DEPENDENCY OF FREQUENCY OF FES MODE

When the temperature increases, the lattice constants in $SrTiO_3$ change and eventually a phase transition to a cubic geometry occurs [3]. To include the effect of the lattice change induced by the temperature in the calculation of the FES mode frequency, we evaluated different 2D potential energy surfaces corresponding to lattice geometries at different temperatures. The temperature dependent lattice parameters used are extracted from the experimental results shown in Fig. S1(b) and rescaled in order to have the same lattice parameter predicted by PBE at $T = 0$ K [3]. In addition, up to 105 K, we decreased AFD angle linearly with the temperature. With the 2D potential energy surface generated by such thermal lattice, we evaluated frequency of FES mode by solving 2D Schrödinger equation. As shown in Fig. S1(c), the FES mode is stiffened as compared to the unchanged lattice results and the stiffening is more significant above 100 K. Even though a stiffening is observed the overall improvement over the results for fixed lattice are minimal, indicating that most of the physics is captured in the $T = 0$ K geometry. The discrepancy with the experimental results for both methods are then attributed to the coupling of the missing phonon modes, rather than the lattice change and quenching of the AFD mode induced by the temperature.

* dongbin.shin@mpsd.mpg.de

† angel.rubio@mpsd.mpg.de

[1] D. T. Colbert and W. H. Miller, The Journal of Chemical Physics **96**, 1982 (1992).

[2] R. M. Wentzcovitch, Phys. Rev. B **44**, 2358 (1991).

[3] R. Loetzsch, A. Lübcke, I. Uschmann, E. Förster, V. Groe, M. Thuerk, T. Koettig, F. Schmidl, and P. Seidel, Appl. Phys. Lett. **96**, 071901 (2010).

[4] R. Wahl, D. Vogtenhuber, and G. Kresse, Phys. Rev. B **78**, 104116 (2008).

TABLE S1. Eigenvector of FES mode and effective mass in atomic Ry unit

	LDA	PBEsol	PBE
Sr	0.03	0.08	0.05
Ti	0.3	0.27	0.26
O_{out}	-0.26	-0.24	-0.26
O_{in}	-0.21	-0.24	-0.21
M_f^{eff}	96532	95821	96958

TABLE S2. Coefficients of 2D potential energy surface with LDA functional

Ry/Å^n	Q_f^{12}	Q_f^{10}	Q_f^8	Q_f^6	Q_f^4	Q_f^2	Q_f^0
Q_c^0	9.5×10^3	-4.5×10^3	-9.3×10^2	-1.1×10^2	2.4×10^1	1.7×10^{-1}	
Q_c^1	-1.1×10^4	4.4×10^3	-7.8×10^2	9.4×10^1	-2.1×10^1	-3.4×10^0	
Q_c^2	3.2×10^4	-8.7×10^3	8.4×10^2	-4.7×10^1	7.8×10^0	2.5×10^{-1}	3.4×10^{-1}
Q_c^3	-2.7×10^5	1.0×10^5	-1.7×10^4	1.3×10^3	4.8×10^1	-2.0×10^{-1}	-3.8×10^{-1}
Q_c^4	1.9×10^5	-1.7×10^5	-4.9×10^4	-6.0×10^3	2.8×10^2	-4.2×10^0	1.4×10^0
Q_c^5	7.0×10^5	-4.2×10^4	-4.8×10^4	8.6×10^3	-4.5×10^2	7.0×10^0	-2.3×10^0

TABLE S3. Coefficients of 2D potential energy surface with PBEsol functional

Ry/Å^n	Q_f^{12}	Q_f^{10}	Q_f^8	Q_f^6	Q_f^4	Q_f^2	Q_f^0
Q_c^0	3.8×10^3	-2.1×10^3	5.1×10^2	-7.2×10^1	1.7×10^1	-2.4×10^{-2}	
Q_c^1	-1.0×10^4	4.6×10^3	-8.8×10^2	1.0×10^2	-1.7×10^1	-2.6×10^0	
Q_c^2	1.4×10^4	-5.2×10^3	7.8×10^2	-6.9×10^1	8.0×10^0	2.0×10^0	3.3×10^{-1}
Q_c^3	-1.4×10^4	4.2×10^3	-4.0×10^2	3.3×10^0	1.2×10^0	-8.9×10^{-1}	-4.3×10^{-1}
Q_c^4	-2.7×10^3	2.3×10^3	-4.3×10^2	2.4×10^1	5.5×10^{-1}	6.4×10^{-2}	-3.4×10^{-1}
Q_c^5	4.8×10^4	-1.9×10^4	2.5×10^3	-9.7×10^1	-4.1×10^0	3.8×10^{-1}	3.7×10^0

TABLE S4. Coefficients of 2D potential energy surface with PBE functional

Ry/Å^n	Q_f^{12}	Q_f^{10}	Q_f^8	Q_f^6	Q_f^4	Q_f^2	Q_f^0
Q_c^0	6.3×10^3	-3.1×10^3	6.8×10^2	-8.6×10^1	2.1×10^1	-2.4×10^{-1}	
Q_c^1	-1.7×10^4	7.0×10^3	-1.2×10^3	1.3×10^2	-2.1×10^1	-2.7×10^0	
Q_c^2	1.8×10^4	-6.0×10^3	8.8×10^2	-8.6×10^1	1.1×10^1	2.1×10^0	3.0×10^{-1}
Q_c^3	-2.9×10^3	-1.1×10^3	3.9×10^2	-4.5×10^1	2.2×10^0	-9.8×10^{-1}	-3.9×10^{-1}
Q_c^4	1.4×10^5	-4.9×10^4	6.4×10^3	-3.6×10^2	8.2×10^0	9.1×10^{-2}	-3.0×10^{-1}
Q_c^5	-4.3×10^5	1.6×10^5	-2.1×10^4	1.3×10^3	-3.9×10^1	6.8×10^{-1}	3.2×10^0

TABLE S5. Coefficients of 2D potential energy surface with HSE06 functional

Ry/Å^n	Q_f^{12}	Q_f^{10}	Q_f^8	Q_f^6	Q_f^4	Q_f^2	Q_f^0
Q_c^0	4.9×10^3	-2.5×10^3	5.5×10^2	-7.4×10^1	2.1×10^1	-2.1×10^{-1}	
Q_c^1	-1.2×10^4	5.5×10^3	-1.1×10^3	1.3×10^2	-2.3×10^1	-2.8×10^0	
Q_c^2	2.0×10^5	-6.6×10^4	8.5×10^3	-5.4×10^2	2.4×10^1	2.1×10^0	3.0×10^{-1}
Q_c^3	-7.3×10^5	2.11×10^5	-2.3×10^4	1.1×10^3	-2.4×10^1	-8.1×10^{-1}	-1.5×10^{-2}
Q_c^4	-1.1×10^6	4.3×10^5	-6.1×10^4	4.0×10^3	-1.2×10^2	1.7×10^0	3.0×10^{-2}
Q_c^5	5.0×10^6	-1.6×10^6	1.9×10^5	-1.0×10^4	2.6×10^2	-2.5×10^0	-1.6×10^0

TABLE S6. The lattice parameter and frequency of ferroeletric soft mode in the tetragonal $SrTiO_3$ with and without quantum fluctuation and elastic effect.

	LDA	PBEsol	PBE	HSE06
a (Å)	3.843	3.882	3.929	3.908
c/a	1.008	1.007	1.005	1.004
δc^{2D} (Å)	0.0041	0.0055	0.018	0.011
c^{2D}/a	1.0091	1.0084	1.0095	1.0068
DFPT (THz)	2.4	-1.5	-3.9	-2.2 [4]
2DSE (THz)	4.1	2.4	0.44	0.83

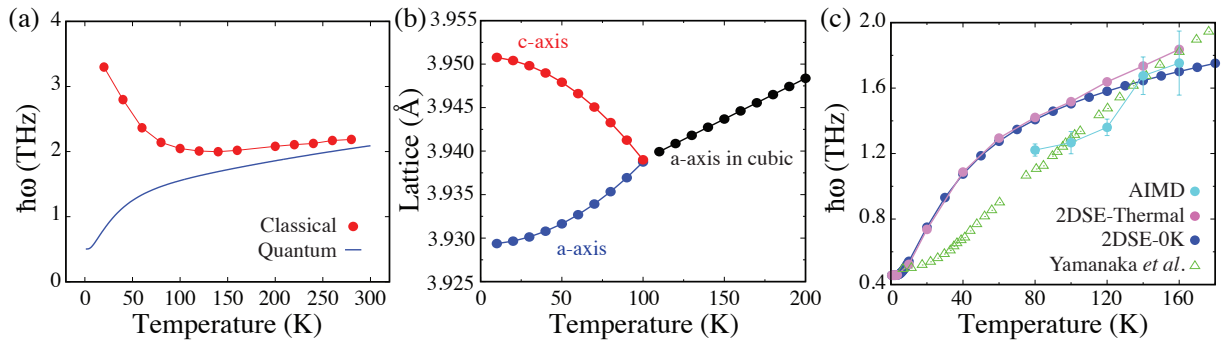

FIG. S1. (a) Temperature dependence of FES mode under classical and quantum description with 2D potential energy surface. (b) Lattice parameter for given temperature evaluated from interpolation of experimental value. (c) Temperature dependence of frequency of FES mode with and without thermal lattice.

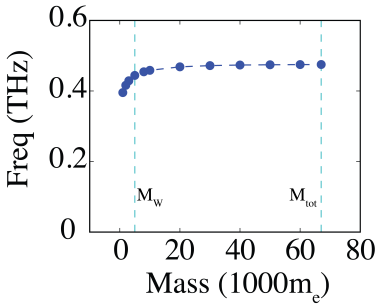

FIG. S2. Variation of frequency of ferroeletric soft mode with respect to lattice mass with PBE functional. The vertical lines indicate the Wentzcovitch-type lattice mass (M_W) and total lattice mass (M_{tot}).